Int. J. Solids Structures Vol. 28, No. 8, pp. 955–974, 1991
Printed in Great Britain.

0020-7683/91 $3.00 + .00

EXACT TRANSIENT SOLUTIONS OF BURIED DYNAMIC POINT FORCES AND DISPLACEMENT JUMPS FOR AN ELASTIC HALF SPACE

CHWAN-HUEI TSAI and CHIEN-CHING MA†
Department of Mechanical Engineering, National Taiwan University, Taipei, Taiwan 10764, Republic of China

(*Received* 29 *May* 1990; *in revised form* 15 *February* 1991)

Abstract—The exact transient closed form solutions for applying time-dependent point forces and displacement jumps at a depth below the surface of an elastic half plane are obtained in this study. A new methodology for constructing the reflected field is proposed and is shown to be both powerful and efficient. The solution of an exponentially distributed loading in the Laplace transform domain at the surface of a half plane is considered as the fundamental solution. The waves reflected from the free surface caused by the incident waves can be constructed by superimposing the fundamental solution. The numerical results of stress and displacement fields during the transient process are obtained and compared with the corresponding static value. It is shown in this study that the dynamic transient solution will approach the static value after the last reflected wave has passed.

1. INTRODUCTION

The propagation of stress waves through an unbounded medium is not a difficult subject. If the boundary is introduced, however, reflected waves will be generated from the free surface, making the problem more complicated. The classical analysis in this area was first proposed by Lamb (1904); he considered the half space subjected to point and line loads on the surface of a semi-infinite half space. Since this early analysis of Lamb, a great many contributions have appeared, pertaining to what is commonly referred to as Lamb's problem. Buried source problems are of considerable interest in seismology and have been studied by many investigators, including Lamb. Nakano (1925) analyzed the buried line dilatation source in a half space, but he failed in generalizing his harmonic steady state results to transient solutions. Lapwood (1949) re-studied Nakano's problem, and later Garvin (1956) also solved Nakano's buried line dilatation source problem by using a suitable distortion of the contour suggested by the work of Cagniard. In Garvin's paper, the numerical results are limited to surface displacement due to a dilatation source, and the generated waves in the medium are incident P waves, reflected PP waves and PS waves.

The three-dimensional problem of a buried vertical point source was studied by Pekeris (1955a,b) and Pekeris and Lifson (1957). Pekeris divided the half space into two regions horizontally along the loading position, and then applied Laplace and Hankel transforms to solve this problem. From the traction-free boundary condition and the continuity requirement at the intersection of the two regions, complicated solutions were represented in integral form and only the surface displacements were obtained numerically. Based on similar methodology, Payton (1967, 1968) solved the displacement of a free surface and an axial line of two-dimensional half space subjected to a buried line source. The suddenly applied normal point load which travels on the surface was first derived by Gakenheimer and Miklowitz (1969). The Laplace and Fourier transforms were employed to solve the problem, and the Cagniard-de Hoop method (1958) was applied to invert the transform.

In this paper, the transient response of applying a point force and displacement jump in an arbitrary direction under the two-dimensional half space is investigated by an alternative methodology, and the exact closed form solutions of the full field will be demonstrated. The two-dimensional static solutions of the stress distribution due to point loads applied within the elastic half plane has been solved by Melan (1932). These solutions were extended and applied to the direct boundary element method for half plane problems

†To whom correspondence should be addressed.

by Telles and Brebbia (1981). The three-dimensional static fundamental solution for the half space has been solved by Mindlin (1936), and its application to the boundary element method has also been established by Nakaguma (1979). From the transient results of this study, it is believed that this analysis will shed some light on the development of the elastodynamic boundary element for half plane problems.

In this investigation, the transient response of buried point forces and displacement jumps in the vertical and horizontal directions of the half surface will be studied in detail. Some solutions have been published by a number of investigators, but none have provided a complete analysis of this problem. A different analytical approach is proposed and is used successfully to obtain the exact transient solution in this study. Fundamental solutions of applying exponentially distributed traction in the Laplace transform domain are established preliminarily in order to construct the more complicated reflected response. From physical considerations, the reflected fields are generated in order to eliminate the stress induced by incident waves in the traction-free surface. For most incident problems, the stress field in the Laplace transform domain (with respect to time) can be represented in an integral form of Laplace inversion (with respect to coordinates), the kernel of which is usually an exponential function. Hence, if the response from applying exponentially distributed traction in the Laplace transform domain can be solved preliminarily, the reflected full field can then be constructed by the superposition method. Because the application of superposition over the new fundamental solution involves only one parameter, it will be more convenient than the superposition of other methods using two parameters. The results described in this paper are exact and are expressed in a simple closed form, each mathematical term representing a physical transient wave. The results of the numerical calculations of stress and displacement are used to investigate the characteristic time during which the transient effect is important.

2. REQUIRED FUNDAMENTAL SOLUTIONS

In conventional studies of transient stress waves, the solution of Lamb's problem for applied point loading at the surface of a half plane was regarded as the fundamental solution. The generation of reflected waves from the free surface can be obtained by superimposing the fundamental solution of Lamb's problem over time and space; hence it involves multiple integrals. Computational inefficiency and complexity can thus be expected. In this paper, an alternative fundamental solution in the Laplace transform domain is proposed. The advantage of using this new fundamental solution is that the superposition process involves only one integral.

Consider a plane strain deformation of half space, with an infinite series of exponential propagation traction force applied on the surface at time $t = 0$. The traction forces can be divided into four categories which contain normal force and tangential force for symmetric and anti-symmetric distribution.

2.1. *Fundamental solution of the symmetric normal traction*

In the case of a half space which is initially at rest, the geometry and coordinate system are shown in Fig. 1. The surface ($x_2 = 0$) is subjected to an infinite series of exponentially distributed normal forces of complex form, which can be represented by the following integral form:

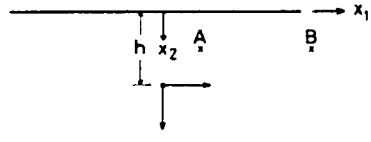

Fig. 1. Configuration and coordinate system of a half plane subjected to an interior dynamic point source.

$$\sigma_{22}^F(x_1,0,t)=\frac{1}{2\pi}\int_{-\infty}^{\infty}\exp\left(-(p_1d_1-p_2d_2)|x_1|+p_1t\right)$$
$$\times\exp\left(i(-(p_2d_1+p_1d_2)|x_1|+p_2t)\right)\mathrm{d}p_2 \quad \text{for} \quad -\infty<x_1<\infty. \quad (1)$$

The physical meaning of (1) is that the loading strength varies in a wave form with an extended velocity of $p_1/(p_1d_1-p_2d_2)$ and is coupled with a harmonic phase variation. If we let variables $p=p_1+ip_2$ and $d=d_1+id_2$, then (1) becomes

$$\sigma_{22}^F(x_1,0,t)=\frac{1}{2\pi i}\int_{p_1-i\infty}^{p_1+i\infty}\mathrm{e}^{-pd|x_1|+pt}\,\mathrm{d}p \quad \text{for} \quad -\infty<x_1<\infty, \quad (2)$$

and the boundary condition of the tangential traction is

$$\sigma_{12}^F(x_1,0,t)=0 \quad \text{for} \quad -\infty<x_1<\infty. \quad (3)$$

The governing equations can be represented by the longitudinal potential ϕ and the shear potential ψ as follows

$$\nabla^2\phi-a^2\ddot{\phi}=0, \quad (4)$$

$$\nabla^2\psi-b^2\ddot{\psi}=0, \quad (5)$$

where

$$a=\sqrt{\frac{\rho}{\gamma+2\mu}}=\frac{1}{v_l}, \quad b=\sqrt{\frac{\rho}{\mu}}=\frac{1}{v_s};$$

a and b are the slowness of the longitudinal wave and the shear wave, μ and ρ are the shear modulus and the mass density, and γ is the Lamé elastic constant. The displacement and stress can be derived from the potentials

$$u_1=\frac{\partial\phi}{\partial x_1}+\frac{\partial\psi}{\partial x_2}, \quad (6)$$

$$u_2=\frac{\partial\phi}{\partial x_2}-\frac{\partial\psi}{\partial x_1}, \quad (7)$$

$$\sigma_{11}=\gamma\nabla^2\phi+2\mu\left(\frac{\partial^2\phi}{\partial x_1^2}+\frac{\partial^2\psi}{\partial x_1\,\partial x_2}\right), \quad (8)$$

$$\sigma_{22}=\gamma\nabla^2\phi+2\mu\left(\frac{\partial^2\phi}{\partial x_2^2}-\frac{\partial^2\psi}{\partial x_1\,\partial x_2}\right), \quad (9)$$

$$\sigma_{12}=\mu\left(2\frac{\partial^2\phi}{\partial x_1\,\partial x_2}-\frac{\partial^2\psi}{\partial x_1^2}+\frac{\partial^2\psi}{\partial x_2^2}\right). \quad (10)$$

This problem can be solved by the application of integral transforms. The one-sided Laplace transform over time and the two-sided Laplace transform over x_1 for a function ϕ is defined by

$$\bar{\phi}^*(\lambda, x_2, p) = \int_{-\infty}^{\infty} e^{-p\lambda x_1} \int_0^{\infty} \phi(x_1, x_2, t) e^{-pt} \, dt \, dx_1. \tag{11}$$

The appropriate expressions for $\bar{\phi}^*$ and $\bar{\psi}^*$ can be represented in the forms

$$\bar{\phi}^* = \Phi(\lambda, x_2, p) e^{-p\alpha x_2}, \tag{12}$$

$$\bar{\psi}^* = \Psi(\lambda, x_2, p) e^{-p\beta x_2}, \tag{13}$$

where

$$\alpha = (a^2 - \lambda^2)^{1/2}, \quad \beta = (b^2 - \lambda^2)^{1/2}.$$

The boundary conditions indicated in (2) and (3) in the Laplace transform domain become

$$\bar{\sigma}_{22}^F(x_1, 0, p) = e^{-pd|x_1|} \quad \text{for} \quad -\infty < x_1 < \infty, \tag{14}$$

$$\bar{\sigma}_{12}^F(x_1, 0, p) = 0 \quad \text{for} \quad -\infty < x_1 < \infty. \tag{15}$$

Equation (14) can be regarded as the exponentially distributed traction in the Laplace domain. Taking the bilateral Laplace transform on x_1 under the restriction of $\mathrm{Re}\,(d \pm \lambda) > 0$, then

$$\bar{\sigma}_{22}^{*F}(\lambda, 0, p) = \frac{2d}{p(d^2 - \lambda^2)}, \tag{16}$$

$$\bar{\sigma}_{12}^{*F}(\lambda, 0, p) = 0. \tag{17}$$

Substituting (12) and (13) into (9), (10), (16) and (17), the unknowns $\Phi(\lambda, x_2, p)$ and $\Psi(\lambda, x_2, p)$ can be solved, and the full field solutions can be obtained. Here, only $\bar{\sigma}_{22}^F$ and $\bar{u}_2^F$ are presented in the Laplace transform domain, as follows:

$$\bar{\sigma}_{22}^F(x_1, x_2, p) = \frac{1}{2\pi i} \int \frac{2d(b^2 - 2\lambda^2)^2}{R(d^2 - \lambda^2)} e^{-p\alpha x_2 + p\lambda x_1} + \frac{8d\alpha\beta\lambda^2}{R(d^2 - \lambda^2)} e^{-p\beta x_2 + p\lambda x_1} \, d\lambda, \tag{18}$$

$$\bar{u}_2^F(x_1, x_2, p) = -\frac{1}{2\pi i} \int \frac{2d\alpha(b^2 - 2\lambda^2)}{\mu p R(d^2 - \lambda^2)} e^{-p\alpha x_2 + p\lambda x_1} + \frac{4d\alpha\lambda^2}{\mu p R(d^2 - \lambda^2)} e^{-p\beta x_2 + p\lambda x_1} \, d\lambda, \tag{19}$$

where R is the Rayleigh wave equation, defined by

$$R = (b^2 - 2\lambda^2)^2 + 4\lambda^2 \alpha\beta.$$

2.2. *Fundamental solution of the anti-symmetric normal traction*

Consider the case in which normal tractions are anti-symmetric with respect to the x_2 axis, then the boundary conditions in the Laplace transform domain are

$$\begin{aligned} \bar{\sigma}_{22}^F(x_1, 0, p) &= e^{pdx_1} \quad \text{for} \quad -\infty < x_1 < 0, \\ &= -e^{-pdx_1} \quad \text{for} \quad 0 < x_1 < \infty, \end{aligned} \tag{20}$$

$$\bar{\sigma}_{12}^F(x_1, 0, p) = 0 \quad \text{for} \quad -\infty < x_1 < \infty. \tag{21}$$

From a procedure similar to the case of symmetric normal traction discussed in Section 2.1, $\bar{\sigma}_{22}^F$ and $\bar{u}_2^F$ can be obtained as

$$\bar{\sigma}^F_{22}(x_1, x_2, p) = \frac{1}{2\pi i}\int \frac{2\lambda(b^2-2\lambda^2)^2}{R(d^2-\lambda^2)} e^{-p\alpha x_2 + p\lambda x_1} + \frac{8\alpha\beta\lambda^3}{R(d^2-\lambda^2)} e^{-p\beta x_2 + p\lambda x_1}\, d\lambda, \quad (22)$$

$$\bar{u}^F_2(x_1, x_2, p) = -\frac{1}{2\pi i}\int \frac{2\alpha\lambda(b^2-2\lambda^2)}{\mu p R(d^2-\lambda^2)} e^{-p\alpha x_2 + p\lambda x_1} + \frac{4\alpha\lambda^3}{\mu p R(d^2-\lambda^2)} e^{-p\beta x_2 + p\lambda x_1}\, d\lambda. \quad (23)$$

2.3. *Fundamental solution of the symmetric tangential traction*

Consider tangential tractions at the surface which are symmetric with respect to the x_2 axis; we have

$$\bar{\sigma}^F_{22}(x_1, 0, p) = 0 \quad \text{for} \quad -\infty < x < \infty, \quad (24)$$

$$\bar{\sigma}^F_{12}(x_1, 0, p) = e^{-pd|x_1|} \quad \text{for} \quad -\infty < x < \infty. \quad (25)$$

The full field solutions of $\bar{\sigma}^F_{22}$ and $\bar{u}^F_2$ in the Laplace transform domain are

$$\bar{\sigma}^F_{22}(x_1, x_2, p) = \frac{1}{2\pi i}\int \frac{-4\beta d\lambda(b^2-2\lambda^2)}{R(d^2-\lambda^2)} e^{-p\alpha x_2 + p\lambda x_1} + \frac{4\beta d\lambda(b^2-2\lambda^2)}{R(d^2-\lambda^2)} e^{-p\beta x_2 + p\lambda x_1}\, d\lambda, \quad (26)$$

$$\bar{u}^F_2(x_1, x_2, p) = \frac{1}{2\pi i}\int \frac{4\alpha\beta d\lambda}{\mu p R(d^2-\lambda^2)} e^{-p\alpha x_2 + p\lambda x_1} - \frac{2d\lambda(b^2-2\lambda^2)}{\mu p R(d^2-\lambda^2)} e^{-p\beta x_2 + p\lambda x_1}\, d\lambda. \quad (27)$$

2.4. *Fundamental solution of the anti-symmetric tangential traction*

When the tangential tractions are anti-symmetric with respect to the x_2 axis, the boundary conditions are

$$\bar{\sigma}^F_{22}(x_1, 0, p) = 0 \quad \text{for} \quad -\infty < x_1 < \infty, \quad (28)$$

$$\bar{\sigma}^F_{12}(x_1, 0, p) = e^{pdx_1} \quad \text{for} \quad -\infty < x_1 < 0$$
$$= -e^{-pdx_1} \quad \text{for} \quad 0 < x_1 < \infty. \quad (29)$$

The full field solutions of $\bar{\sigma}^F_{22}$ and $\bar{u}^F_2$ are

$$\bar{\sigma}^F_{22}(x_1, x_2, p) = \frac{1}{2\pi i}\int \frac{-4\beta\lambda^2(b^2-2\lambda^2)}{R(d^2-\lambda^2)} e^{-p\alpha x_2 + p\lambda x_1} + \frac{4\beta\lambda^2(b^2-2\lambda^2)}{R(d^2-\lambda^2)} e^{-p\beta x_2 + p\lambda x_1}\, d\lambda, \quad (30)$$

$$\bar{u}^F_2(x_1, x_2, p) = \frac{1}{2\pi i}\int \frac{4\alpha\beta\lambda^2}{\mu p R(d^2-\lambda^2)} e^{-p\alpha x_2 + p\lambda x_1} - \frac{2\lambda^2(b^2-2\lambda^2)}{\mu p R(d^2-\lambda^2)} e^{-p\beta x_2 + p\lambda x_1}\, d\lambda. \quad (31)$$

3. TRANSIENT SOLUTIONS OF BURIED POINT SOURCES

In this study, two types of point forces and displacement jumps are considered. The direction of any applied point force and displacement jump can be divided into directions which are perpendicular and parallel to the free surface. Any solution of arbitrary direction can be constructed by the combination of the solutions of these two directions. The transient elastodynamic problems of half space can be solved by superposition of the incident and reflected waves. The full field solution of the incident field is denoted by the superscript *I* and the reflected field by superscript *R*. The incident field is the response from loading applied on an unbounded medium, and the reflected field is the solution of loading applied to a traction-free surface to eliminate the stress induced by the incident wave.

3.1. *Vertical concentrated force*

Consider an isotropic linear elastic half space; the elastic medium occupies the region $-\infty \leqslant x_1 \leqslant \infty, x_2 \geqslant 0$. Initially, the body is stress-free and at rest. At time $t = 0$, a vertical concentrated force along the positive x_2 axis is applied at the position of distance h under the free surface. The time dependence of the loading is represented by $\sigma_0 f(t)$ with the geometry and coordinate system shown in Fig. 1. The point force is represented by

$$\sigma_{22}(x_1, h^+, t) - \sigma_{22}(x_1, h^-, t) = -\sigma_0 f(t)\delta(x_1), \tag{32}$$

where $f(t)$ vanishes for $t < 0$. Incident fields in the Laplace transform domain can be represented as (Achenbach, 1973)

$$\bar{\sigma}^I_{22} = \frac{\sigma_0 \operatorname{sgn}(h-x_2)}{2\pi i}\int pF(p)\left[\frac{b^2-2\lambda^2}{2b^2}\mathrm{e}^{-p\alpha|x_2-h|-p\lambda|x_1|} + \frac{\lambda^2}{b^2}\mathrm{e}^{-p\beta|x_2-h|-p\lambda|x_1|}\right]\mathrm{d}\lambda, \tag{33}$$

$$\bar{\sigma}^I_{12} = \frac{\sigma_0 \operatorname{sgn}(x_1)}{2\pi i}\int pF(p)\left[\frac{-\alpha\lambda}{b^2}\mathrm{e}^{-p\alpha|x_2-h|-p\lambda|x_1|} + \frac{\lambda(b^2-2\lambda^2)}{2b^2\beta}\mathrm{e}^{-p\beta|x_2-h|-p\lambda|x_1|}\right]\mathrm{d}\lambda, \tag{34}$$

$$\bar{u}^I_2 = \frac{\sigma_0}{2\pi i\mu}\int F(p)\left[\frac{\alpha}{2b^2}\mathrm{e}^{-p\alpha|x_2-h|-p\lambda|x_1|} + \frac{\lambda^2}{2b^2\beta}\mathrm{e}^{-p\beta|x_2-h|-p\lambda|x_1|}\right]\mathrm{d}\lambda. \tag{35}$$

For convenience, we define the following functions:

$$E_1(\lambda) = \mathrm{e}^{-p\alpha|x_2-h|+p\lambda x_1}, \quad E_2(\lambda) = \mathrm{e}^{-p\beta|x_2-h|+p\lambda x_1}, \tag{36}$$

$$A_{11}(\lambda) = \operatorname{sgn}(h-x_2)\frac{b^2-2\lambda^2}{2b^2}, \quad A_{12}(\lambda) = \operatorname{sgn}(h-x_2)\frac{\lambda^2}{b^2}, \tag{37}$$

$$B_{11}(\lambda) = \frac{\alpha}{2b^2}, \quad B_{12}(\lambda) = \frac{\lambda^2}{2b^2\beta}. \tag{38}$$

The sgn (x_1) function represents the symbol + or − depending on the sign of variable x_1; $F(p)$ is the Laplace transform of $f(t)$.

The stresses $\bar{\sigma}_{22}$ and $\bar{\sigma}_{12}$, which should be applied at $x_2 = 0$ to eliminate the incident wave, can be deduced from (33) and (34) in the Laplace transform domain, that is

$$\bar{\sigma}_{22} = -\frac{\sigma_0}{2\pi i}\int pF(p)\left[\frac{b^2-2\lambda^2}{2b^2}\mathrm{e}^{-p\alpha h-p\lambda|x_1|} + \frac{\lambda^2}{b^2}\mathrm{e}^{-p\beta h-p\lambda|x_1|}\right]\mathrm{d}\lambda, \tag{39}$$

$$\bar{\sigma}_{12} = -\frac{\sigma_0 \operatorname{sgn}(x_1)}{2\pi i}\int pF(p)\left[-\frac{\alpha\lambda}{b^2}\mathrm{e}^{-p\alpha h-p\lambda|x_1|} + \frac{\lambda(b^2-2\lambda^2)}{2b^2\beta}\mathrm{e}^{-p\beta h-p\lambda|x_1|}\right]\mathrm{d}\lambda. \tag{40}$$

From (39) and (40), we can see that the applied tractions in space, in order to eliminate the incident wave, are represented by the function $\mathrm{e}^{-p\lambda|x_1|}$. Since the solutions of applying traction $\mathrm{e}^{-pd|x_1|}$ at the surface have been solved in Section 2, the reflected field induced by applying loading of (39) and (40) can be constructed by superposition and replacing λ by d. When we combine eqns (18), (19), (30) and (31), the reflected waves for $\bar{\sigma}_{22}$ in the Laplace transform domain can be expressed as follows:

$$\bar{\sigma}_{22}^{R}(x_1,x_2,p) = -\frac{\sigma_0 pF(p)}{2\pi i}\int\left[\frac{b^2-2d^2}{2b^2}e^{-p\alpha^* h}+\frac{d^2}{b^2}e^{-p\beta^* h}\right]$$

$$\times\frac{1}{2\pi i}\int\frac{2d(b^2-2\lambda^2)^2}{R(d^2-\lambda^2)}e^{-p\alpha x_2+p\lambda x_1}+\frac{8d\alpha\beta\lambda^2}{R(d^2-\lambda^2)}e^{-p\beta x_2+p\lambda x_1}\,d\lambda\,dd$$

$$+\frac{\sigma_0 pF(p)}{2\pi i}\int\left[-\frac{d\alpha^*}{b^2}e^{-p\alpha^* h}+\frac{d(b^2-2d^2)}{2b^2\beta^*}e^{-p\beta^* h}\right]$$

$$\times\frac{1}{2\pi i}\int\frac{-4\beta\lambda^2(b^2-2\lambda^2)}{R(d^2-\lambda^2)}e^{-p\alpha x_2+p\lambda x_1}+\frac{4\beta\lambda^2(b^2-2\lambda^2)}{R(d^2-\lambda^2)}e^{-p\beta x_2+p\lambda x_1}\,d\lambda\,dd, \quad (41)$$

where

$$\alpha^* = (a^2-d^2)^{1/2}, \quad \beta^* = (b^2-d^2)^{1/2}.$$

From the restriction of $\mathrm{Re}\,(d\pm\lambda) > 0$, the integral path of d must be located at the right-hand side of λ. Thus, if the integral path of d is changed to go through the imaginary axis, the integrals of pole at $d = \lambda$ or $-\lambda$ must be considered. Since (41) is an odd function of d, the integral along the imaginary axis will vanish. Finally, from Cauchy's integral theorem, the original integrals of (41) can be further reduced as

$$\bar{\sigma}_{22}^{R}(x_1,x_2,p) = \frac{\sigma_0 pF(p)}{2\pi i}\int_\Gamma\sum_{j=3}^{6}A_{1j}(\lambda)E_j(\lambda)\,d\lambda, \quad (42)$$

where

$$A_{13}(\lambda) = \frac{-(b^2-2\lambda^2)^3+4\alpha\beta\lambda^2(b^2-2\lambda^2)}{2b^2R}, \quad A_{14}(\lambda) = \frac{-4\alpha\beta\lambda^2(b^2-2\lambda^2)}{b^2R},$$

$$A_{15}(\lambda) = \frac{-2\lambda^2(b^2-2\lambda^2)^2}{b^2R}, \quad A_{16}(\lambda) = \frac{\lambda^2(b^2-2\lambda^2)^2-4\alpha\beta\lambda^4}{b^2R}, \quad (43)$$

$$E_3(\lambda) = e^{-p\alpha(x_2+h)+p\lambda x_1}, \quad E_4(\lambda) = e^{-p\beta x_2-p\alpha h+p\lambda x_1},$$

$$E_5(\lambda) = e^{-p\alpha x_2-p\beta h+p\lambda x_1}, \quad E_6(\lambda) = e^{-p\beta(x_2+h)+p\lambda x_1}. \quad (44)$$

Displacement $\bar{u}_2$ can also be obtained as

$$\bar{u}_2^{R}(x_1,x_2,p) = \frac{\sigma_0 F(p)}{2\pi i\mu}\int_\Gamma\sum_{j=3}^{6}B_{1j}(\lambda)E_j(\lambda)\,d\lambda, \quad (45)$$

where

$$B_{13}(\lambda) = \frac{\alpha(b^2-2\lambda^2)^2-4\beta\alpha^2\lambda^2}{2b^2R}, \quad B_{14}(\lambda) = \frac{2\alpha\lambda^2(b^2-2\lambda^2)}{b^2R},$$

$$B_{15}(\lambda) = \frac{2\alpha\lambda^2(b^2-2\lambda^2)}{b^2R}, \quad B_{16} = \frac{4\alpha\beta\lambda^4-\lambda^2(b^2-2\lambda^2)^2}{2b^2\beta R}. \quad (46)$$

3.2. *Horizontal concentrated force*

Consider the same geometry and coordinate system as shown in Fig. 1, the loading is applied horizontally and has the same direction as the positive x_1 axis. The incident fields in the Laplace transform domain will be

$$\bar{\sigma}^{I}_{22} = \frac{\sigma_0}{2\pi i}\int pF(p)\sum_{j=1}^{2} A_{2j}(\lambda)E_j(\lambda)\,d\lambda, \tag{47}$$

$$\bar{u}^{I}_{2} = \frac{\sigma_0}{2\pi i\mu}\int F(p)\sum_{j=1}^{2} B_{2j}(\lambda)E_j(\lambda)\,d\lambda, \tag{48}$$

where

$$A_{21}(\lambda) = \frac{\lambda(b^2-2\lambda^2)}{2b^2\alpha}, \quad A_{22}(\lambda) = \frac{\beta\lambda}{b^2}, \tag{49}$$

$$B_{21}(\lambda) = \operatorname{sgn}(h-x_2)\frac{\lambda}{2b^2}, \quad B_{22}(\lambda) = -\operatorname{sgn}(h-x_2)\frac{\lambda}{2b^2}. \tag{50}$$

Following the same arguments as in Section 3.1, the reflected fields in the Laplace transform domain can be obtained as

$$\bar{\sigma}^{R}_{22}(x_1,x_2,p) = \frac{\sigma_0 pF(p)}{2\pi i}\int_{\Gamma}\sum_{j=3}^{6} A_{2j}(\lambda)E_j(\lambda)\,d\lambda, \tag{51}$$

$$\bar{u}^{R}_{2}(x_1,x_2,p) = \frac{\sigma_0 F(p)}{2\pi i\mu}\int_{\Gamma}\sum_{j=3}^{6} B_{2j}(\lambda)E_j(\lambda)\,d\lambda, \tag{52}$$

where

$$A_{23}(\lambda) = \frac{-\lambda(b^2-2\lambda^2)^3+4\alpha\beta\lambda^3(b^2-2\lambda^2)}{2b^2\alpha R}, \quad A_{24}(\lambda) = \frac{-4\beta\lambda^3(b^2-2\lambda^2)}{b^2R},$$
$$A_{25}(\lambda) = \frac{2\beta\lambda(b^2-2\lambda^2)^2}{b^2R}, \quad A_{26}(\lambda) = \frac{4\alpha\beta^2\lambda^3-\beta\lambda(b^2-2\lambda^2)^2}{b^2R}. \tag{53}$$

$$B_{23}(\lambda) = \frac{\lambda(b^2-2\lambda^2)^2-4\alpha\beta\lambda^3}{2b^2R}, \quad B_{24}(\lambda) = \frac{2\lambda^3(b^2-2\lambda^2)}{b^2R},$$
$$B_{25}(\lambda) = \frac{-2\alpha\beta\lambda(b^2-2\lambda^2)}{b^2R}, \quad B_{26}(\lambda) = \frac{-4\alpha\beta\lambda^3+\lambda(b^2-2\lambda^2)^2}{2b^2R}. \tag{54}$$

3.3. *Vertical concentrated displacement jump*

Consider a concentrated displacement jump which is emitted from distance h under the free surface suddenly applied at time $t = 0$ along the vertical direction. The displacement jump can be represented by

$$u_2(x_1,h^+,t) - u_2(x_1,h^-,t) = u_0 f(t)\delta(x_1). \tag{55}$$

The incident fields in the Laplace transform domain are

$$\bar{\sigma}^I_{22} = \frac{\mu u_0}{2\pi i}\int p^2 F(p) \sum_{j=1}^{2} A_{3j}(\lambda) E_j(\lambda)\,\mathrm{d}\lambda, \tag{56}$$

$$\bar{u}^I_2 = \frac{u_0}{2\pi i}\int pF(p) \sum_{j=1}^{2} B_{3j}(\lambda) E_j(\lambda)\,\mathrm{d}\lambda, \tag{57}$$

where

$$A_{31} = -\frac{(b^2-2\lambda^2)^2}{2b^2\alpha}, \quad A_{32} = -\frac{2\beta\lambda^2}{b^2}, \tag{58}$$

$$B_{31} = -\operatorname{sgn}(h-x_2)\frac{b^2-2\lambda^2}{2b^2}, \quad B_{32} = -\operatorname{sgn}(h-x_2)\frac{\lambda^2}{b^2}. \tag{59}$$

The reflected fields can be obtained as follows:

$$\bar{\sigma}^R_{22}(x_1, x_2, p) = \frac{\mu u_0 p^2 F(p)}{2\pi i}\int_\Gamma \sum_{j=3}^{6} A_{3j}(\lambda) E_j(\lambda)\,\mathrm{d}\lambda, \tag{60}$$

$$\bar{u}^R_2(x_1, x_2, p) = \frac{u_0 pF(p)}{2\pi i}\int_\Gamma \sum_{j=3}^{6} B_{3j}(\lambda) E_j(\lambda)\,\mathrm{d}\lambda, \tag{61}$$

where

$$A_{33}(\lambda) = \frac{(b^2-2\lambda^2)^4 - 4\alpha\beta\lambda^2(b^2-2\lambda^2)^2}{2b^2\alpha R}, \quad A_{34}(\lambda) = \frac{4\beta\lambda^2(b^2-2\lambda^2)^2}{b^2 R},$$
$$A_{35}(\lambda) = \frac{4\beta\lambda^2(b^2-2\lambda^2)^2}{b^2 R}, \qquad A_{36}(\lambda) = \frac{8\alpha\beta^2\lambda^4 - 2\beta\lambda^2(b^2-2\lambda^2)^2}{b^2 R}. \tag{62}$$

$$B_{33}(\lambda) = \frac{-(b^2-2\lambda^2)^3 + 4\alpha\beta\lambda^2(b^2-2\lambda^2)}{2b^2 R}, \quad B_{34}(\lambda) = -\frac{2\lambda^2(b^2-2\lambda^2)^2}{b^2 R},$$
$$B_{35}(\lambda) = -\frac{4\alpha\beta\lambda^2(b^2-2\lambda^2)}{b^2 R}, \qquad B_{36}(\lambda) = \frac{\lambda^2(b^2-2\lambda^2)^2 - 4\alpha\beta\lambda^4}{b^2 R}. \tag{63}$$

3.4. *Horizontal concentrated displacement jump*

If the displacement jump is in the horizontal x_1 direction, the incident fields in the Laplace transform domain are

$$\bar{\sigma}^I_{22} = \frac{\mu u_0}{2\pi i}\int p^2 F(p) \sum_{j=1}^{2} A_{4j}(\lambda) E_j(\lambda)\,\mathrm{d}\lambda, \tag{64}$$

$$\bar{u}^I_2 = \frac{u_0}{2\pi i}\int pF(p) \sum_{j=1}^{2} B_{4j}(\lambda) E_j(\lambda)\,\mathrm{d}\lambda, \tag{65}$$

where

$$A_{41}(\lambda) = -\frac{(b^2-2\lambda^2)(b^2-2\alpha^2)}{2b^2\alpha}, \quad A_{42}(\lambda) = \frac{2\beta\lambda^2}{b^2}, \tag{66}$$

$$B_{41}(\lambda) = -\operatorname{sgn}(h-x_2)\frac{(b^2-2\alpha^2)}{2b^2}, \quad B_{42}(\lambda) = \operatorname{sgn}(h-x_2)\frac{\lambda^2}{b^2}. \tag{67}$$

The reflected fields are

$$\bar{\sigma}_{22}^R(x_1, x_2, p) = \frac{\mu u_0 p^2 F(p)}{2\pi i}\int_\Gamma \sum_{j=3}^{6} A_{4j}(\lambda)E_j(\lambda)\,\mathrm{d}\lambda, \tag{68}$$

$$\bar{u}_2^R(x_1, x_2, p) = \frac{u_0 p F(p)}{2\pi i}\int_\Gamma \sum_{j=3}^{6} B_{4j}(\lambda)E_j(\lambda)\,\mathrm{d}\lambda, \tag{69}$$

where

$$\begin{aligned}
A_{43}(\lambda) &= \frac{(b^2-2\lambda^2)^3(b^2-2\alpha^2) - 4\alpha\beta\lambda^2(b^2-2\lambda^2)(b^2-2\alpha^2)}{2b^2\alpha R}, \\
A_{44}(\lambda) &= \frac{4\beta\lambda^2(b^2-2\lambda^2)(b^2-2\alpha^2)}{b^2 R}, \\
A_{45}(\lambda) &= \frac{-4\beta\lambda^2(b^2-2\lambda^2)^2}{b^2 R}, \quad A_{46}(\lambda) = \frac{-8\alpha\beta^2\lambda^4 + 2\beta\lambda^2(b^2-2\lambda^2)^2}{b^2 R},
\end{aligned} \tag{70}$$

$$\begin{aligned}
B_{43}(\lambda) &= \frac{-(b^2-2\lambda^2)^2(b^2-2\alpha^2) + 4\alpha\beta\lambda^2(b^2-2\alpha^2)}{2b^2 R}, \\
B_{44}(\lambda) &= \frac{-2\lambda^2(b^2-2\lambda^2)(b^2-2\alpha^2)}{b^2 R}, \\
B_{45}(\lambda) &= \frac{4\alpha\beta\lambda^2(b^2-2\lambda^2)}{b^2 R}, \quad B_{46}(\lambda) = \frac{4\alpha\beta\lambda^4 - \lambda^2(b^2-2\lambda^2)^2}{b^2 R}.
\end{aligned} \tag{71}$$

The remaining task is to evaluate the inverse transforms of the above expressions for reflected fields.

4. CAGNIARD–DE HOOP METHOD

The full field solutions represented in the previous section are in the Laplace transform domain. By the application of the Cagniard–de Hoop method of Laplace inversion, the path of integration is deformed in such a way that the inverse Laplace transform of the integral along the new distortion path of integration can be readily obtained. From the following elementary property of the one-sided Laplace transform,

$$\mathscr{L}^{-1}\left\{\int_{t_1}^{\infty} \mathrm{e}^{-pt} g(t)\,\mathrm{d}t\right\} = g(t)H(t-t_1), \tag{72}$$

the inversion of the two transforms can be operated at one time. We will consider the stress σ_{22} in some detail. For the first term of (42), consider now a new integration variable t defined by

$$\alpha(x_2+h) - \lambda x_1 = t. \tag{73}$$

Equation (73) can be solved for λ to yield

$$\lambda_{\Gamma_\pm}(r_2,\theta_2,t) = -\frac{t}{r_2}\cos\theta_2 \pm i\sqrt{\frac{t^2}{r_2^2}-a^2}\sin\theta_2, \tag{74}$$

where

$$r_2^2 = (x_2+h)^2+x_1^2, \quad \cos\theta_2 = \frac{x_1}{r_2}, \quad \sin\theta_2 = \frac{x_2+h}{r_2}.$$

This represents essentially a transformation from the t-plane to the λ-plane which changes the path of integration Γ to $\Gamma_\pm$. In the λ-plane, (74) describes a hyperbola as shown in Fig. 2a. When $t = ar_2 = T_{PP}$, the imaginary part of λ vanishes, and the vertex of the hyperbola is defined by $\lambda = -a\cos\theta_2$. As time t increases from ar_2 to ∞, the integral path approaches a straight line in the λ-plane having a slope of $\tan\theta_2$ and passing through the origin. The hyperbola paths Γ_+ and Γ_- are shown in Fig. 2a. This path will be a suitable deformed integral contour to replace the original integral path Γ. The first term of (42) becomes

$$\bar{\sigma}_{22} = \sigma_0 pF(p)\frac{1}{\pi}\int_{T_{PP}}^{\infty} \mathrm{Im}\left[A_{13}(\lambda_3)\frac{\partial\lambda_3}{\partial t}\right]e^{-pt}\,dt, \tag{75}$$

where $\lambda_3 = \lambda_{\Gamma_+}(r_2,\theta_2,t)$ of (74). From the convolution property of (72), the inversion of the Laplace transform in the time domain is

$$\sigma_{22}(x_1,x_2,t) = \sigma_0\int_{T_{PP}}^{t}\frac{df(t')}{dt'}\,\mathrm{Im}\left[A_{13}(\lambda_3)\frac{\partial\lambda_3}{\partial\tau}\right]d\tau, \tag{76}$$

where $t' = t-\tau$ and λ_3 becomes a function of τ. The wave front arrives at time $t = T_{PP}$, with the subscript PP denoting the primary wave reflected by the incident primary wave.

As the Cagniard-de Hoop method is employed on the second term of (42), let

$$\beta x_2+\alpha h-\lambda x_1 = t. \tag{77}$$

We cannot solve analytically for λ, but from the formulation of a quartic algebraic equation, the roots can be obtained explicitly. When the imaginary part of λ vanishes, the correspondence time t is denoted by T_{PS}. As t extends from T_{PS} to ∞, the integral path extends from a hyperbola curve and approaches a straight line, as shown in Fig. 2a. The vertex of the hyperbola is located on the real axis between the branch points at $-a$ and a. The second term of (42) then becomes

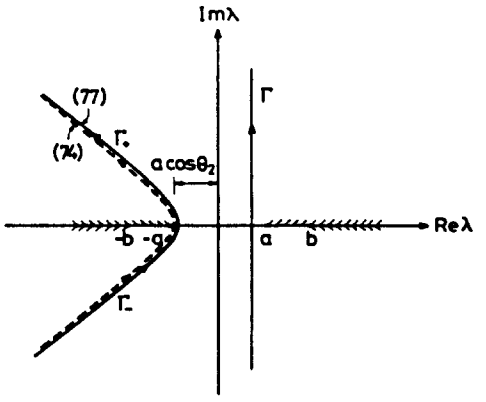

Fig. 2a. Deformed integral contour as presented in (74) and (77).

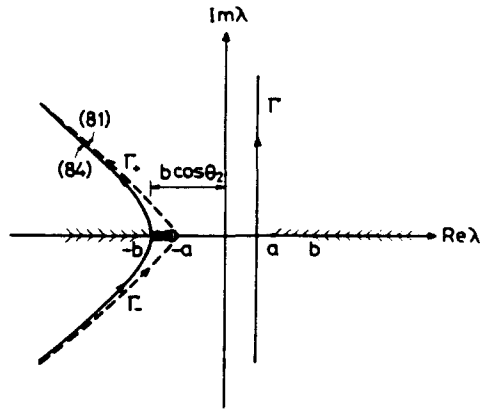

Fig. 2b. Deformed integral contour as presented in (81) and (84).

$$\bar{\sigma}_{22}(x_1, x_2, p) = \sigma_0 p F(p) \frac{1}{\pi} \int_{T_{PS}}^{\infty} \mathrm{Im}\left[A_{14}(\lambda_4) \frac{\partial \lambda_4}{\partial t}\right] \mathrm{e}^{-pt}\, \mathrm{d}t. \tag{78}$$

The inversion of the Laplace transform is

$$\sigma_{22}(x_1, x_2, t) = \sigma_0 \int_{T_{PS}}^{t} \frac{\mathrm{d}f(t')}{\mathrm{d}t'} \mathrm{Im}\left[A_{14}(\lambda_4) \frac{\partial \lambda_4}{\partial \tau}\right] \mathrm{d}\tau, \tag{79}$$

where λ_4 is the root of (77) and T_{PS} denotes the time at which the reflected secondary wave front generated by the incident primary wave arrives. $\partial\lambda_4/\partial\tau$ can be obtained by taking a derivative on (77), which yields

$$\frac{\partial \lambda_4}{\partial \tau} = -1 \Big/ \left(\frac{\lambda_4 x_2}{\beta} + \frac{\lambda_4 h}{\alpha} + x_1\right). \tag{80}$$

A similar procedure is applied to the third term of (42); let

$$\alpha x_2 + \beta h - \lambda x_1 = t. \tag{81}$$

Following the same argument as described in (77)–(80), this becomes

$$\sigma_{22}(x_1, x_2, t) = \frac{\sigma_0}{\pi} \int_{T_{SP}}^{t} \frac{\mathrm{d}f(t')}{\mathrm{d}t'} \mathrm{Im}\left[A_{15}(\lambda_5) \frac{\partial \lambda_5}{\partial \tau}\right] \mathrm{d}\tau, \tag{82}$$

where λ_5 is the root of (81), and

$$\frac{\partial \lambda_5}{\partial \tau} = -1 \Big/ \left(\frac{\lambda_5 x_2}{\alpha} + \frac{\lambda_5 h}{\beta} + x_1\right). \tag{83}$$

T_{SP} denotes the time at which the reflected primary wave induced by the incident secondary wave arrives. The deformed integral path is shown in Fig. 2b. The intersection with the real axis is always located in the region between $-a$ and a.

Now let us consider the fourth term of (42). When we let

$$\beta(x_2 + h) - \lambda x_1 = t, \tag{84}$$

(84) can be solved for λ explicitly to yield

$$\lambda_{\Gamma_\pm}(r_2,\theta_2,t) = -\frac{t}{r_2}\cos\theta_2 \pm i\sqrt{\frac{t^2}{r_2^2}-b^2}\sin\theta_2. \tag{85}$$

When $t = br_2$, it indicates the time at which the reflected secondary wave front generated by the incident secondary wave arrives, and is denoted by T_{SS}. The deformed integral contour is shown in Fig. 2b. If $b|\cos\theta_2| > a$, an additional integral path from $t = T_{HD}$ to $t = T_{SS}$, which embraces the branch cut, must be considered. In this integral interval, λ is real and is represented as follows:

$$\lambda_{H_\pm}(r_2,\theta_2,t) = -\frac{t}{r_2}\cos\theta_2 + \mathrm{sgn}(x_1)\sqrt{b^2-\frac{t^2}{r_2^2}}\sin\theta_2 \quad \text{for} \quad T_{HD} < t < T_{SS}, \tag{86}$$

where

$$T_{HD} = ar_2|\cos\theta_2| + r_2\sqrt{b^2-a^2}\sin\theta_2. \tag{87}$$

This additional integral path represents the head wave induced by the incident secondary wave, where the wave front of the head wave arrives at time $t = T_{HD}$. The final form of the fourth term of (42) becomes

$$\sigma_{22}(x_1,x_2,t) = \frac{\sigma_0}{\pi}\int_{T_{HD}}^{t}\frac{\mathrm{d}f(t')}{\mathrm{d}t'}\,\mathrm{Im}\left[A_{16}(\lambda_7)\frac{\partial\lambda_7}{\partial\tau}\right]H(T_{SS}-\tau)\,\mathrm{d}\tau + \frac{\sigma_0}{\pi}\int_{T_{SS}}^{t}\frac{\mathrm{d}f(t')}{\mathrm{d}t'}\,\mathrm{Im}\left[A_{16}(\lambda_6)\frac{\partial\lambda_6}{\partial\tau}\right]\mathrm{d}\tau, \tag{88}$$

where $\lambda_6 = \lambda_{\Gamma_+}(r_2,\theta_2,\tau)$ of (85), and $\lambda_7 = \lambda_{H_+}(r_2,\theta_2,\tau)$ of (86). The other stress and displacement reflected fields presented in the previous section can be derived in a similar manner, thus the details are omitted here. If the loading history $f(t)$ is a Heaviside function $H(t)$, the exact explicit transient solutions can be obtained and are summarized as follows.

4.1. *For point force*

$$\sigma_{22}(x_1,x_2,t) = \frac{\sigma_0}{\pi}\sum_{j=1}^{6}\mathrm{Im}\left[A_{ij}(\lambda_j)\frac{\partial\lambda_j}{\partial t}\right]H(t-T_j) + \frac{\sigma_0}{\pi}\mathrm{Im}\left[A_{i6}(\lambda_7)\frac{\partial\lambda_7}{\partial t}\right](H(t-T_7)-H(t-T_6)), \tag{89}$$

$$u_2(x_1,x_2,t) = \frac{\sigma_0}{\pi\mu}\sum_{j=1}^{6}\int_{T_j}^{t}\mathrm{Im}\left[B_{ij}(\lambda_j)\frac{\partial\lambda_j}{\partial\tau}\right]\mathrm{d}\tau H(t-T_j) + \frac{\sigma_0}{\pi\mu}\int_{T_7}^{t}\mathrm{Im}\left[B_{i6}(\lambda_7)\frac{\partial\lambda_7}{\partial\tau}\right]H(T_6-\tau)\,\mathrm{d}\tau H(t-T_7), \tag{90}$$

where i is valid for 1 and 2, representing the cases of the vertical and horizontal concentrated forces, respectively.

4.2. *For displacement jump*

$$\sigma_{22}(x_1,x_2,t)=\frac{\mu u_0}{\pi}\frac{\mathrm{d}}{\mathrm{d}t}\sum_{j=1}^{6}\mathrm{Im}\left[A_{ij}(\lambda_j)\frac{\partial\lambda_j}{\partial t}\right]H(t-T_j)$$
$$+\frac{\mu u_0}{\pi}\frac{\mathrm{d}}{\mathrm{d}t}\mathrm{Im}\left[A_{i6}(\lambda_7)\frac{\partial\lambda_7}{\partial t}\right](H(t-T_7)-H(t-T_6)), \quad (91)$$

$$u_2(x_1,x_2,t)=\frac{u_0}{\pi}\sum_{j=1}^{6}\mathrm{Im}\left[B_{ij}(\lambda_j)\frac{\partial\lambda_j}{\partial t}\right]H(t-T_j)$$
$$+\frac{u_0}{\pi}\mathrm{Im}\left[B_{i6}(\lambda_7)\frac{\partial\lambda_7}{\partial t}\right](H(t-T_7)-H(t-T_6)), \quad (92)$$

where i is valid for 3 and 4, representing the cases of the vertical and horizontal concentrated displacement jumps, respectively. The j values represent the P, S, PP, PS, SP, SS and HD waves in the sequence of 1–7. The last terms of (89)–(92) represent the head wave which only exists in the region $b|\cos\theta_2|>a$. The functions λ_1 and λ_2 are obtained from the incident P and S waves and are defined as

$$\lambda_1(t)=-\frac{t}{r_1}\cos\theta_1+i\sqrt{\frac{t^2}{r_1^2}-a^2}\sin\theta_1,$$
$$\lambda_2(t)=-\frac{t}{r_1}\cos\theta_1+i\sqrt{\frac{t^2}{r_1^2}-b^2}\sin\theta_1, \quad (93)$$

where

$$r_1^2=(x_2-h)^2+x_1^2,\quad \cos\theta_1=\frac{x_1}{r_1},\quad \sin\theta_1=\frac{|x_2-h|}{r_1}.$$

5. NUMERICAL RESULTS

A structural steel of Poisson's ratio $\nu=0.3$ and $b=1.8708a$ is chosen for the numerical calculation. When the point forces and displacement jumps are applied suddenly at the point $(0,h)$, the induced wave fronts of incident and reflected waves are as shown in Fig. 3. The figure also illustrates the processes for the development of the reflected waves. Using

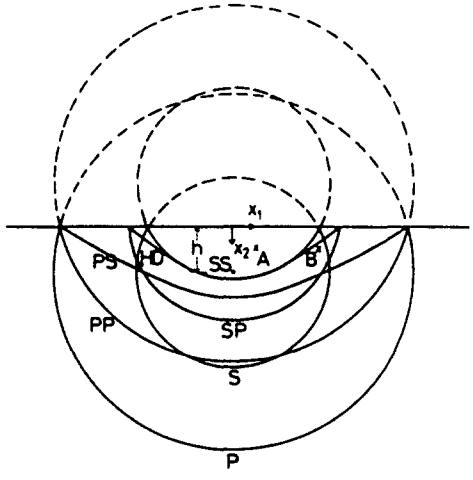

Fig. 3. Wave fronts of the incident waves and reflected waves at $t/ah=4$.

the concept of image method, on the opposite side there is an image source from which the reflected PP and SS waves emit. When the PP wave is generated, the traction-free condition at the free boundary will not be satisfied; thus the coupled PS wave must be generated at the same time. After some time delay, the reflected SP wave induced by the incident shear S wave will be coupled with a head wave HD in order to satisfy the traction-free boundary condition. Finally, the reflected SS wave is emitted following the head wave. The wave fronts of P, S and PP, SS are cylindrical curves emitted from the source and image, the HD wave is an inclined straight line, and PS and SP wave fronts are smooth curves which are constructed by numerical calculations. The head wave only occurs in the region of $a/b < \cos\theta_2$. In this section, numerical results for applying the Heaviside function of time dependence for point sources in the interior of a half space are evaluated. The field points are selected at $(0.5h, 0.5h)$ denoted by A and $(2h, 0.5h)$ by B. Transient responses of σ_{22} and u_2 are obtained and are presented in Figs 4–7. The point B will be subjected to the disturbance of the head wave. The static solutions are also shown in these figures. The transient solution approaches the static solution as time increases beyond theoretical bounds.

If we apply point force of Heaviside function dependence, the stress fields behave as the square root singularity at the wave front, except in the case of the head wave. The displacement fields are continuous at the wave fronts. For the case of applying displacement jump of Heaviside function dependence, the singularity of the stress fields at the wave front will be one order stronger than the case of the point force.

Telles and Brebbia (1981) obtained the static results of a half space when applying static point force. The transient analysis in this study tends toward the corresponding static value, as expected. The static value of the applied displacement jump under half space is not available in the published literature, but the numerical calculations of the static value are not difficult. Generally speaking, the dynamic transient effect is important under dynamic loading conditions. The dynamic response of stress in the transient period is much greater than its static value. In the transient period, the tensile or compressive effect will change radically when the reflected wave arrives. When the SS wave passes the field point, the field value of stress or displacement will very rapidly tend toward the static value. Table 1 shows the ratio of the dynamic value to the static value after the SS wave has passed.

Another particularly interesting phenomenon observed in the present work is the onset and development of the Rayleigh wave disturbance as x_1/h increases. At the far field, i.e. a large value of x_1, the effect of the Rayleigh pole at the deformed integral contour of the Cagniard–de Hoop method must be considered. The Rayleigh wave will become significant when x_1/h is larger than 10, and a large displacement disturbance on the free surface will be generated as the Rayleigh wave arrives. The vertical displacement is shown in Fig. 8 for various times t/ah, and it clearly shows the birth of Rayleigh wave. The Rayleigh wave suffers no attenuation and remains essentially unchanged in shape.

6. CONCLUSION

The stresses and displacements generated by the application of a point force and displacement jump to an elastic half space comprise the basic solution for the half space.

Table 1. Comparisons of the transient dynamic values and static values of point A after SS wave has passed

	$\sigma_{22}/\sigma_{22}^{st}$				u_2/u_2^{st}			
	Load				Load			
t/ah	(1)	(2)	(3)	(4)	(1)	(2)	(3)	(4)
5	1.526	1.104	0.987	0.967	1.150	1.332	0.990	0.982
6	1.343	1.061	0.993	0.980	1.096	1.233	0.997	0.994
7	1.243	1.037	0.996	0.988	1.067	1.172	1.000	0.998
8	1.180	1.023	0.998	0.992	1.049	1.132	1.002	1.000
9	1.140	1.016	0.999	0.995	1.038	1.105	1.003	1.000
10	1.105	1.012	1.000	0.996	1.032	1.085	1.003	1.000

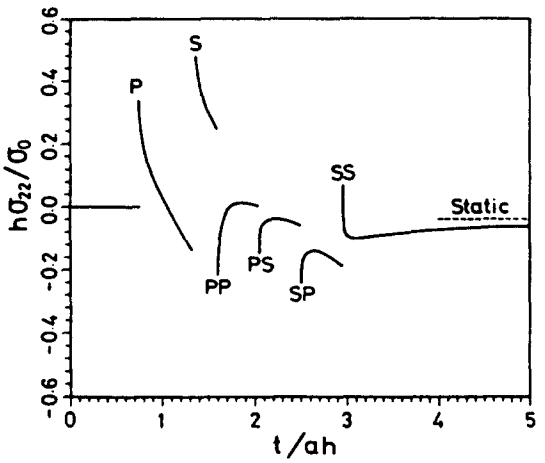

Fig. 4a. Transient normal stress σ_{22} of point A subjected to vertical point force.

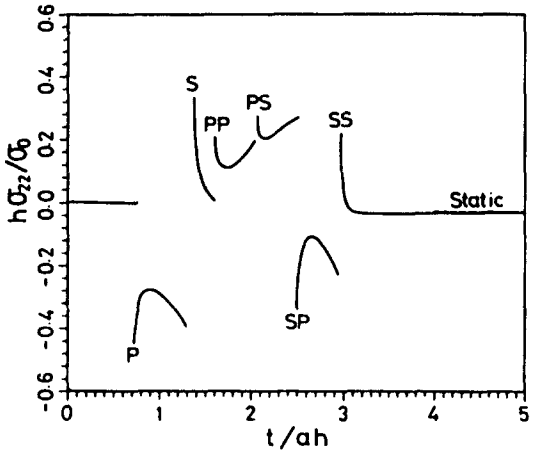

Fig. 4b. Transient normal stress σ_{22} of point A subjected to horizontal point force.

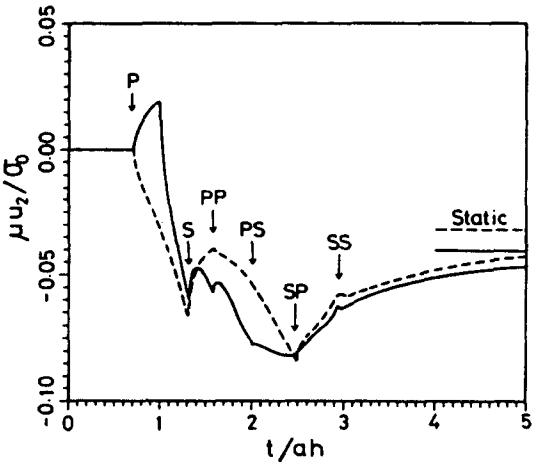

Fig. 4c. Transient relative displacement u_2 of point A to the origin subjected to vertical and horizontal point forces.

In this study, a new methodology and fundamental solution are proposed and are shown to be a powerful tool for constructing the complicated reflected waves. The Cagniard–de Hoop inverse method is used, enabling us to investigate in detail the structure of the wave pattern. The complete solutions of the Green functions for a half space subjected to a

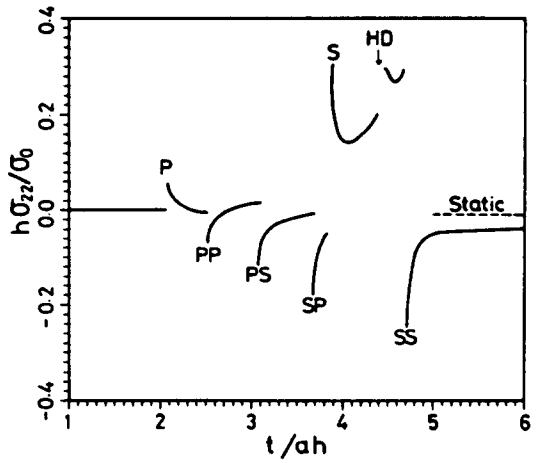

Fig. 5a. Transient normal stress σ_{22} of point B subjected to vertical point force.

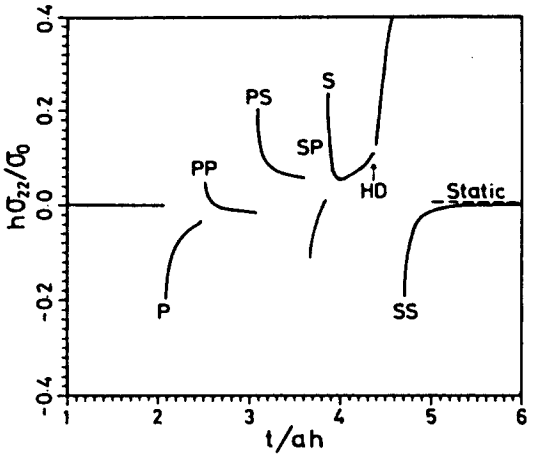

Fig. 5b. Transient normal stress σ_{22} of point B subjected to horizontal point force.

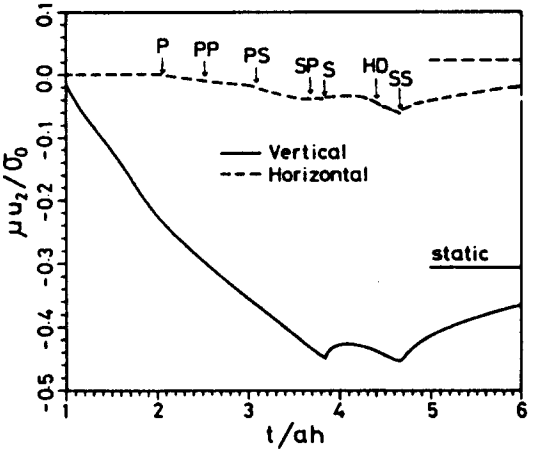

Fig. 5c. Transient relative displacement u_2 of point B to the origin subjected to vertical and horizontal point forces.

dynamic point source are presented in an exact closed form. The present results provide valuable fundamental solutions which can be used to solve more difficult elastodynamic transient problems in half space by a boundary element numerical method.

In order to investigate the characteristic time after which the transient effect can be

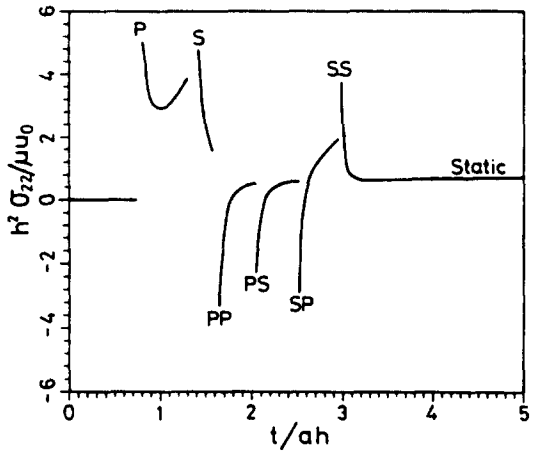

Fig. 6a. Transient normal stress σ_{22} of point A subjected to vertical displacement jump.

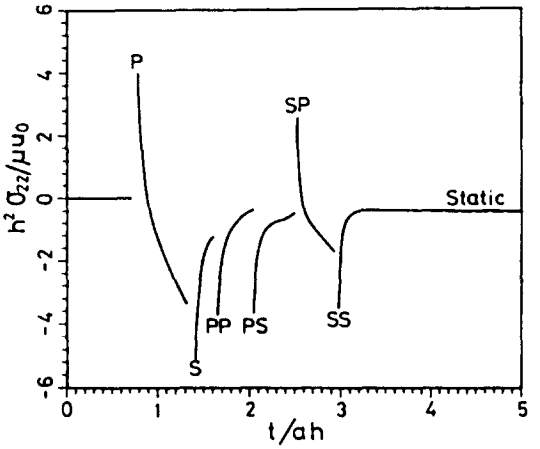

Fig. 6b. Transient normal stress σ_{22} of point A subjected to horizontal displacement jump.

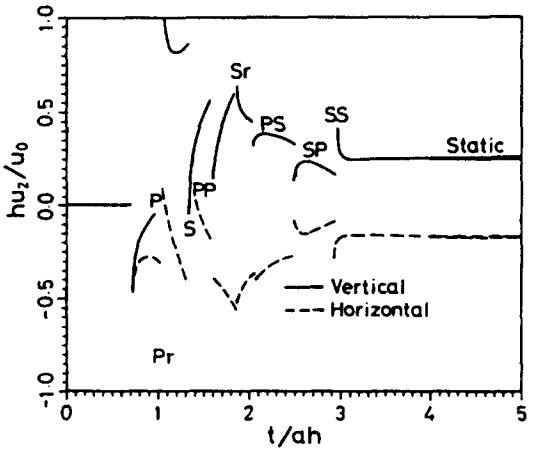

Fig. 6c. Transient relative displacement u_2 of point A to the origin subjected to vertical and horizontal displacement jumps.

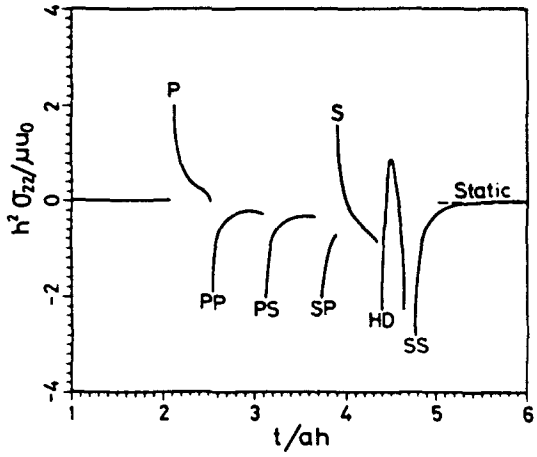

Fig. 7a. Transient normal stress σ_{22} of point B subjected to vertical displacement jump.

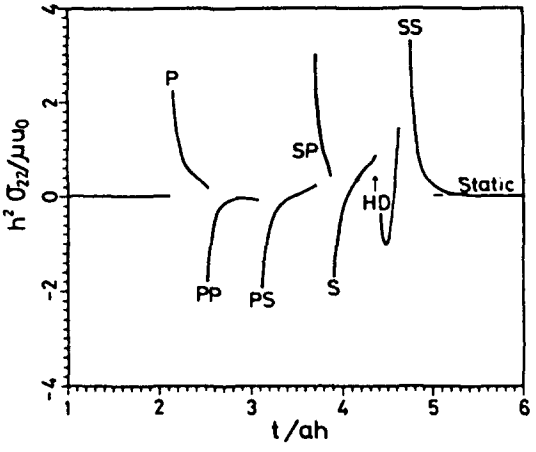

Fig. 7b. Transient normal stress σ_{22} of point B subjected to horizontal displacement jump.

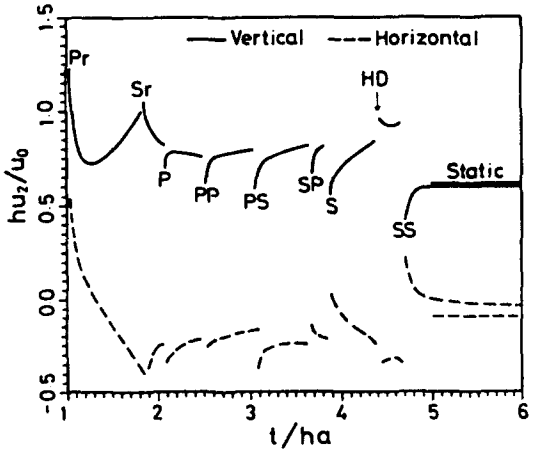

Fig. 7c. Transient relative displacement u_1 of point B to the origin subjected to vertical and horizontal displacement jumps.

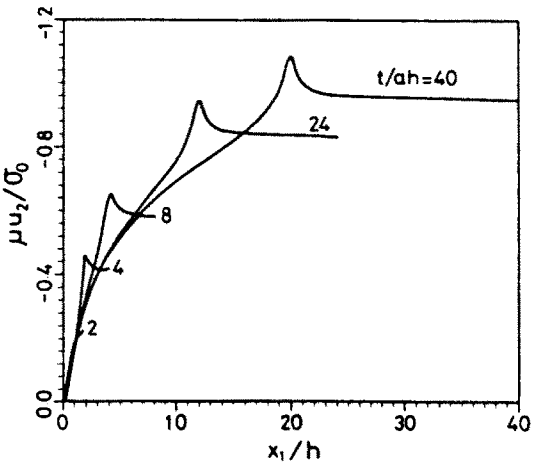

Fig. 8. Transient vertical displacement u_2 of free surface related to the origin from a vertical point force.

neglected, numerical results of stress and displacement based on the transient analysis are presented and compared to the corresponding static solution. It is found that the dynamic transient solution approaches the static value very quickly after the last reflected wave (SS wave) has passed the field point.

Acknowledgement—The financial support of the authors by the National Science Council, Republic of China, through Grant NSC 79-0401-E002-36 is gratefully acknowledged.

REFERENCES

Achenbach, J. D. (1973). *Wave Propagation in Elastic Solids*. North-Holland, New York.

de Hoop, A. T. (1958). Representation theorems for the displacement in an elastic solid and their application to elastodynamic diffraction theory. Doctoral Dissertation, Technische Hogeschool, Delft.

Gakenheimer, D. C. and Miklowitz, J. (1969). Transient excitation of an elastic half space by a point load traveling on the surface. *J. Appl. Mech.* **36**, 505–515.

Garvin, W. W. (1956). Exact transient solution of the buried line source problem. *Proc. R. Soc. Lond.* **A234**, 528–541.

Lamb, H. (1904). On the propagation of tremors over the surface of an elastic solid. *Phil. Trans. R. Soc. Lond.* **A203**, 1–42.

Lapwood, E. R. (1949). *Phil. Trans. R. Soc. Lond.* **A242**, 63–100.

Melan, E. (1932). Der Spannungszustand der durch eine Einzelkraft in innern beanspruchten Halbscheibe. *Z. Angew. Math. Mech.* **12**, 343–346.

Mindlin, R. D. (1936). Force at a point in the interior of a semi-infinite solid. *Physics* **7**, 195–202.

Nakaguma, R. K. (1979). Three dimensional elastostatics using the boundary element method. Ph.D. Thesis, University of Southampton.

Nakano, H. (1925). *Jap. J. Astr. Geophys.* **2**, 233.

Payton, R. G. (1967). Transient motion of an elastic half-space due to a moving surface line load. *Int. J. Engng Sci.* **5**, 49–79.

Payton, R. G. (1968). Epicenter motion of an elastic half-space due to buried stationary and moving line sources. *Int. J. Solids Structures* **4**, 287–300.

Pekeris, C. L. (1955a). The seismic surface pulse. *Proc. Natn Acad. Soc.* **41**, 469–480.

Pekeris, C. L. (1955b). The seismic buried pulse. *Proc. Natn Acad. Soc.* **41**, 629–638.

Pekeris, C. L. and Lifson, H. (1957). Motion of the surface of a uniform elastic half-space produced by a buried pulse. *J. Acoust. Soc. Am.* **29**, 1233–1238.

Telles, J. C. F. and Brebbia, C. A. (1981). Boundary element solution for half-plane problems. *Int. J. Solids Structures* **17**, 1149–1158.